GEOPHYSICAL RESEARCH LETTERS, VOL. 40, 2489–2494, doi:10.1002/grl.50505, 2013

Field-aligned current reconfiguration and magnetospheric response to an impulse in the interplanetary magnetic field B_Y component

F. D. Wilder,[1] S. Eriksson,[1] H. Korth,[2] J. B. H. Baker,[3] M. R. Hairston,[4] C. Heinselman,[5] and B. J. Anderson[2]

Received 2 April 2013; revised 22 April 2013; accepted 24 April 2013; published 6 June 2013.

[1] When the interplanetary magnetic field (IMF) is dawnward or duskward, magnetic merging between the IMF and the geomagnetic field occurs near the cusp on the dayside flanks of the magnetosphere. During these intervals, flow channels in the ionosphere with velocities in excess of 2 km/s have been observed, which can deposit large amounts of energy into the high-latitude thermosphere. In this study, we analyze an interval on 5 April 2010 where there was a strong dawnward impulse in the IMF, followed by a gradual decay in IMF magnitude at constant clock angle. Data from the Sondrestrom incoherent scatter radar and the Defense Meteorological Satellite Program spacecraft were used to investigate ionospheric convection during this interval, and data from the Active Magnetospheric and Planetary Electrodynamics Response Experiment (AMPERE) were used to investigate the associated Field-Aligned Current (FAC) system. Additionally, data from AMPERE were used to investigate the time response of the dawnside FAC pair. We find there is a delay of approximately 1.25 h between the arrival of the dawnward IMF impulse at the magnetopause and strength of the dawnward FAC pair, which is comparable to substorm growth and expansion time scales under southward IMF. Additionally, we find at the time of the peak FAC, there is evidence of a reconfiguring four-sheet FAC system in the morning local time sector of the ionosphere. Additionally, we find an inverse correlation between the dawn FAC strength and both the solar wind Alfvénic Mach number and the SYM-H index. No statistically significant correlation between the FAC strength and the solar wind dynamic pressure was found. **Citation:** Wilder, F. D., S. Eriksson, H. Korth, J. B. H. Baker, M. R. Hairston, C. Heinselman, and B. J. Anderson (2013), Field-aligned current reconfiguration and magnetospheric response to an impulse in the interplanetary magnetic field B_Y component, *Geophys. Res. Lett.*, *40*, 2489–2494, doi:10.1002/grl.50505.

[1]Laboratory of Atmospheric and Space Physics, The University of Colorado at Boulder, Boulder, Colorado, USA.
[2]The Johns Hopkins University Applied Physics Laboratory, Laurel, Maryland, USA.
[3]Bradley Department of Electrical and Computer Engineering, Virginia Tech, Blacksburg, Virginia, USA.
[4]William B. Hanson Center for Space Sciences, University of Texas at Dallas, Richardson, Texas, USA.
[5]SRI International, Menlo Park, California, USA.

Corresponding author: F. D. Wilder, Laboratory of Atmospheric and Space Physics, The University of Colorado at Boulder, Boulder, CO, USA. (frederick.wilder@lasp.colorado.edu)

0094-8276/13/10.1002/grl.50505

1. Introduction

[2] When the interplanetary magnetic field (IMF) is dominated by its dawn-dusk component (B_Y), it reconnects with the geomagnetic field at high latitudes on the dawn or dusk magnetospheric flanks [*Friis-Christensen et al.*, 1972]. Recent efforts to improve satellite drag prediction in Low Earth Orbit have additionally found that during intervals of large IMF B_Y, anomalous upwelling of neutral gas can occur in the dayside, high-latitude thermosphere [*Lühr et al.*, 2004; *Crowley et al.*, 2010]. This upwelling usually coincides with regions of intense downward Poynting flux that contain fast ionospheric **E**x**B** flow channels flanked by strong oppositely directed field-aligned currents (FACs) [*Eriksson et al.*, 2008; *Crowley et al.*, 2010; *Knipp et al.*, 2011]. These flow channels have been shown to map to the reconnection region on the high-latitude magnetospheric flanks [*Li et al.*, 2011; *Wilder et al.*, 2012b].

[3] Previous studies of extreme ionosphere-thermosphere energy deposition from the magnetosphere during IMF B_Y-dominant conditions have focused on steady state conditions, for which the IMF magnitude was large for several hours [*Crowley et al.*, 2010; *Knipp et al.*, 2011; *Wilder et al.*, 2012b]. While these have been valuable in providing a framework in which thermospheric upwelling in the cusp region can be predicted based on average solar wind conditions, more analysis needs to be done to understand the time response of the magnetosphere-ionosphere-thermosphere system to transient IMF features. In the present study, we investigate an event on 5 April 2010, when there was a −21 nT impulse in the IMF B_Y component that slowly returned to zero and maintained a steady IMF clock angle over the course of 8.3 h. Using FAC data from the Active Magnetosphere and Planetary Electrodynamics Response Experiment (AMPERE) and convection data from the Sondrestrom incoherent scatter radar as well as the Defense Meteorological Satellite Program (DMSP), we examine the MLT distribution of an intense reconfiguring FAC pattern and the associated fast-flow channel in the morning sector in response to the IMF impulse. Additionally, we investigate the time response of the peak upward and downward FAC strength near MLT dawn. We find that there is a delay of 1.25 h between the IMF B_Y impulse at the magnetopause and the peak FACs near MLT dawn.

2. Data Analysis and Results

2.1. Solar Wind and Geophysical Conditions

[4] Figure 1 shows the SYM-H index [*Wanliss and Showalter*, 2006] and solar wind and IMF conditions observed by the ACE spacecraft [*Stone et al.*, 1997] and spacecraft B of

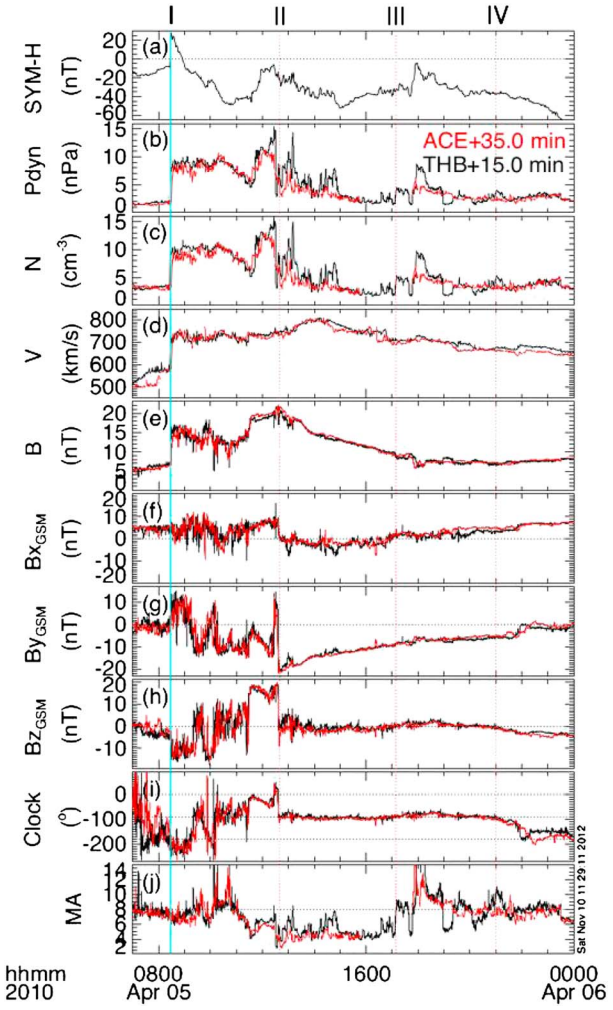

Figure 1. Geomagnetic and solar wind conditions for 5 April 2010: (a) Sym-H index, solar wind (b) dynamic pressure, (c) plasma number density, (d) bulk velocity, IMF (e) magnitude, (f) B_X, (g) B_Y, (h) B_Z, (i) clock angle, and (j) solar wind Alfvénic Mach number. The black and red lines represent data from ACE and THEMIS-B, respectively. Time I is the pressure pulse in the IMF, which was propagated to the magnetopause using the increase in SYM-H. Time II is the negative impulse in IMF B_Y. Time III indicates a return from low-to-nominal *MA* conditions. Time IV indicates the start of a southward turning of the IMF.

the THEMIS mission (THB) [*Angelopoulos*, 2008] after 7 UT on 5 April 2010. During the 12–18 UT interval, the average locations of ACE and THB in Geocentric Solar Ecliptic (GSE) coordinates were (238.6, −35.6, −23.5) R_E and (100.4, 66.6, −2.0) R_E, respectively. At 8:27 UT, a solar wind dynamic pressure pulse encountered the Earth's magnetopause, leading to a sudden increase in the SYM-H index. ACE and THB observed this pressure pulse 35 and 15 min, respectively, prior to the SYM-H sudden impulse. These delays were used to propagate the ACE and THB data to the Earth.

[5] After several hours of fluctuating southward and then northward IMF, the IMF suddenly turned dawnward at ~12:39 UT, with the B_Y component reaching −21 nT and the clock angle equal to −88.5°. The IMF B_Y then slowly decayed until the IMF B_Z component began to turn negative at approximately 21 UT. Additionally, during 4.5 h of this interval, the Alfvénic Mach number (*MA*) in the solar wind was significantly smaller than the nominal value of 8. This can allow sunward convection on open-field lines in the magnetosphere, as the JxB force from a near-cusp or flank reconnection site can significantly exceed the magnetosheath dynamic pressure. During the afternoon B_Y-dominated interval after 12:40 UT, THB observed significant fluctuations in *MA* that were not observed at ACE. This interval with an "impulse" and ensuing decay in IMF B_Y at steady IMF clock angle will be the focus of the present study.

2.2. The 2-D Ionospheric FAC Patterns and Associated Plasma Convection

[6] In order to examine the FAC distribution, the present study uses data from AMPERE. AMPERE uses attitude magnetometer data from the constellation of over 70 Iridium satellites obtained at 20-s cadence per satellite to produce global maps of magnetic perturbations associated with large-scale FACs [*Anderson et al.*, 2000]. To obtain the large-scale FAC distribution, the magnetic field perturbations are fitted to a spherical harmonic expansion to obtain spatially uniform maps of magnetic perturbations from which the FACs are derived using the technique described by *Waters et al.* [2001]. A complete refresh of the magnetic perturbation distribution is obtained every 10 min, commensurate with the inter-spacecraft separation. FAC maps derived from lower time-resolution Iridium data have been used in a variety of scientific studies [e.g., *Anderson et al.*, 2005, 2008; *Korth et al.*, 2005, 2010; *Eriksson et al.*, 2008]. FAC distributions from high time-resolution AMPERE data are available since 2010 and have been used to study the thermospheric response to the northward IMF interval on 5 April 2010 [*Wilder et al.*, 2012a], as well as the storm response of the Region-1 FACs during other time periods [*Clausen et al.*, 2012].

[7] Figure 2 shows four AMPERE FAC patterns for 5 April 2010 at (a) 13:20 UT, (b) 13:50 UT, (c) 14:30 UT and (d) 16:30 UT. At 13:20 UT, which was 40 min after the impulse in IMF B_Y, there is a FAC pair in the pre-noon sector at high latitudes, with the upward current being an extension of the duskside region 1 current, and the downward current being what is commonly referred to as the "cusp" or "region 0" current, which is known to be associated with a strong IMF B_Y component [*Potemra*, 1994]. In the 13:50 UT pattern, there is another current pair in the early dawn sector, with the downward and upward current having polarity similar to the Region 1 and 2 FACs, respectively. Additionally, the cusp current pair has weakened. There is some evidence that along the 9 MLT meridian, there is a four-sheet FAC system [*Yamauchi et al.*, 1993; *Taguchi et al.*, 1993; *Ohtani et al.*, 1995] that can be associated with complex flow patterns and field topologies [*Watanabe and Sofko*, 2009]. It should be noted that while the fitted Birkeland current maps show this signature and local time overlap of the strong current pairs observed at distinctly different latitudes in the adjacent satellite planes is likely, no direct AMPERE observations were obtained in the local time range, where the four-current sheet structure is most prominent. Then, at 14:30 UT, the FAC system has weakened, and while there is evidence of the four-sheet system along the 10 MLT meridian, there is also evidence that the dawnside region 1 current has begun to connect with the noon region 0 current. Finally, at 16:30, the dawnside region 1 current and the high-latitude region 0 current have merged. Additionally, the dawnside region 2 current has weakened significantly.

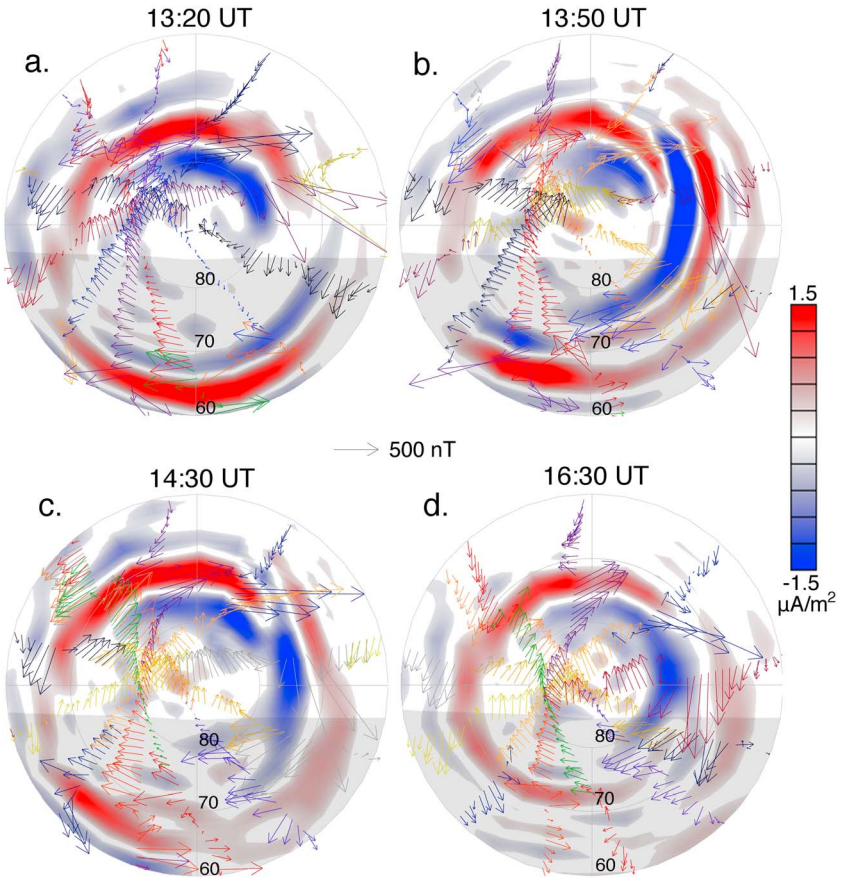

Figure 2. AMPERE FAC patterns on 5 April 2010 at (a) 13:20 UT, (b) 13:50 UT, (c) 14:30 UT, and (d) 16:30 UT. Positive current is upward and arrows indicate raw magnetic residuals from the Iridium constellation that contributed to the pattern. The plots are in AACGM MLAT-MLT format with magnetic noon at the top of the page and the lowest latitude circle at 60°. The shaded region represents the nightside of the day-night terminator.

[8] Ionospheric plasma convection associated with the cusp and dawnside current pair during the FAC reconfiguration can be determined using data from the DMSP drift meter [*Rich and Hairston*, 1994], which passes close to the dawn sector, and the Sondrestrom incoherent scatter radar, which made observations in the near noon sector. Figure 3 shows Sondrestrom velocity vectors and average AMPERE FAC patterns for the duration of two DMSP passes. For the F15 pass at 13:52 UT (top), flows in excess of 2 km/s are observed at each of the two major current pairs. Unlike the F15 pass, for the F16 pass at 14:27 UT (bottom), SSJ/4 particle data were available, and the open-closed boundary was able to be determined in a manner consistent with past studies [*Redmon et al*., 2010; *Wilder et al*., 2012b]. During this interval, flows are still seen in excess of 2 km/s. Additionally, the fastest flows observed by the F16 spacecraft appear to be on open-field lines. Because of the sunward direction of these flows, they are resisted by the magnetosheath flow and must be maintained by a significant Lorentz force. Since the DMSP F16 spacecraft skimmed the cusp current system, this implies that the fast-flow channel extending across the noon meridian is driven by magnetic reconnection between the IMF and geomagnetic field lines on the dawnside flank [*Li et al*., 2011; *Wilder et al*., 2012b]. Therefore, the sunward flow in the morning sector cannot be thought of as typical return flow with its corresponding region 1/region 2 FAC system such as in the *Dungey* [1961] cycle. The origin of the flow channel near local dawn will be discussed in more detail in the following sections.

2.3. The Time-Dependent Response of Dawn Sector FAC Strength to the Impulse in IMF B_Y

[9] The FAC patterns and convection observations in Figure 3 suggest that the reconfiguring current system shown in Figure 2 is associated with intense eastward-directed zonal flows in both the dawn sector and past local noon with velocities exceeding 2 km/s. In the past, flow channels exhibiting velocities of this magnitude have been shown to coincide with extreme levels of Joule heating that can produce "anomalous" upwelling of thermospheric neutral gas in the dayside polar cap [*Crowley et al*., 2010; *Wilder et al*., 2012b]. In order to predict extreme Joule heating, a better understanding of the temporal response of these intense FACs to transient solar wind and IMF features such as the one after 12:40 UT are needed.

[10] Figure 4 shows time series of the SYM-H index, the IMF B_Y component and solar wind *MA* observed by THB, and the maximum and minimum FAC values observed by AMPERE in the dawn sector current pair for 5–8 MLT. The latitudes of the maximum and minimum FAC at 7 MLT are shown. The AMPERE FAC maxima and minima

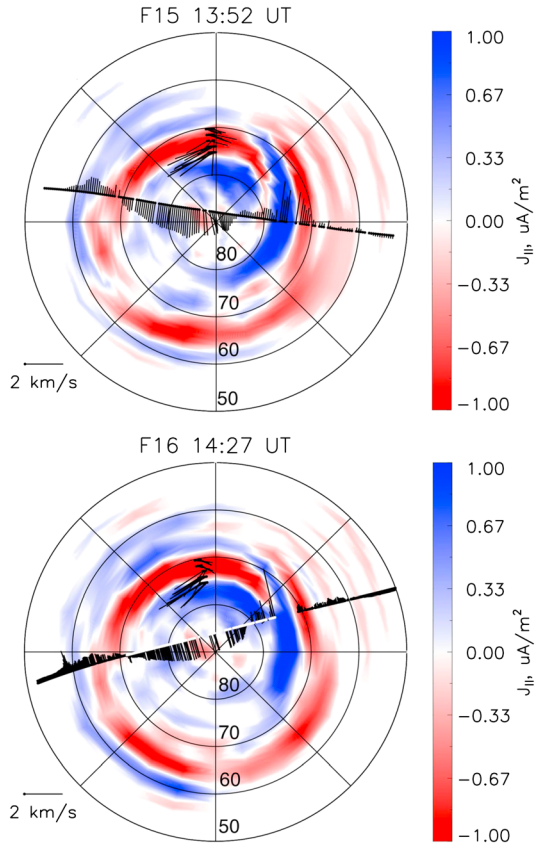

Figure 3. Average FAC maps during two DMSP satellite passes on 5 April 2010 using 30 min of data accumulation: (top) the DMSP F15 pass beginning at 13:52 UT and (bottom) the DMSP F16 pass beginning at 14:27 UT. Black arrows indicate velocity measurements from the DMSP spacecraft and the Sondrestrom incoherent scatter radar. For the F16 pass, regions with open and closed field lines are represented by white and black dots, respectively. Flows in excess of 2 km/s are observed between 70° and 80° MLAT extending from 6 MLT past 12 MLT during both DMSP passes.

time series between 5 and 8 MLT all peak shortly after 14:00 UT, with an average time lag of 1.25 h between the impulse in the IMF B_Y component and the FAC peak magnitude. Coinciding with this peak, the downward current sheet at 7 MLT reached its minimum latitude extent, and the maxima of the upward and downward current sheets were separated by less than 5° latitude. As the magnitude of the IMF B_Y component decreased, the peak current values decreased, and the upward and downward current sheets separated. We note that the integrated absolute value of the FAC (not shown) along each MLT meridian also showed a time lag of approximately 1.25 h. This suggests that there is also an enhancement in the total electromagnetic energy deposited into the dawn-sector ionosphere.

[11] In comparing the peak current with the SYM-H index, as the current increases in magnitude, SYM-H turns increasingly negative. Additionally, during the time period where the FAC strength is growing, the solar wind *MA* is lower than the nominal value of 8. One would expect this, as at higher solar wind *MA*, the magnetosheath *MA* will also increase, which can suppress magnetic reconnection at high latitudes due to flow shear across the magnetopause current sheet [*Cassak*, 2011, and references therein]. Additionally, higher solar wind *MA* conditions can increase the plasma beta in the magnetosheath, which can lead to a suppression of reconnection due to diamagnetic drifts at the magnetopause current sheet [e.g., *Lavraud and Borovsky*, 2008; *Swisdak et al.*, 2010]. *Eriksson and Rastätter* [2013] also used MHD simulations to predict that cusp-region flow channels under IMF B_Y-dominant conditions would be more prominent at lower solar wind *MA*. To provide a more quantitative analysis of these two trends, we compute the Spearman rank correlation coefficient between these quantities and the FAC system [*Spearman*, 1904]. The solar wind *MA* correlates with the peak FAC for the four MLTs shown with an average of −0.43 for the maximum and −0.47 for the minimum. The SYM-H index correlates with an average of −0.41 for the minimum and −0.37 for the maximum, respectively. The minimum and maximum current correlates with the IMF B_Y with an average value of 0.59. All of these correlations pass a significance test against the null hypothesis at the 99% confidence level and were calculated without lagging any of the variables in time. The peak FAC magnitude correlates best with the IMF B_Y, which is to be expected. The correlations between the peak FAC magnitude and the solar wind *MA* and SYM-H appear to be comparable. This demonstrates that there is a complex combination of internal and external driving associated with the FAC system observed here, with significant time lags in place. For example, the peak

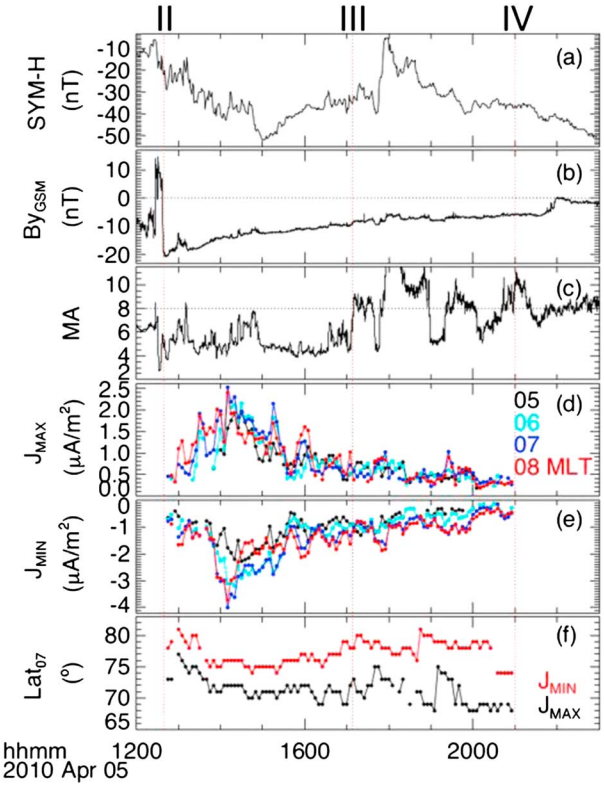

Figure 4. Time series of (a) SYM-H, (b) IMF B_Y, (c) solar wind *MA* observed by THB, (d) maximum, (e) minimum AMPERE FAC values for 5–8 MLT, and (f) the latitude of the minimum and maximum FAC at 7 MLT. FAC values are color coded by MLT. Note that the upward and downward current are plotted on different scales. Vertical dotted lines correspond to times II, II, and IV from Figure 1.

current lags the impulse in IMF B_Y by 1.25 h. Additionally, the SYM-H index turns most negative 50 min after the peak FAC. This makes sense if one considers enhanced convection precedes an enhancement of the ring current. We interpret the correlations to imply that while the IMF B_Y impulse drives the system, and the solar wind *MA* may impact the effectiveness of reconnection at high latitudes. The time lag in the dawn FAC magnitude is likely due to internal processes that also lead to the enhancement of the ring current and the minima of the SYM-H index.

3. Summary and Discussion

[12] The present study investigated the response of the dayside FAC system to an impulse in the IMF B_Y to −21 nT, followed by a gradual decay in magnitude with steady clock angle. We showed that this impulse led to a restructuring of high latitude FACs, as well as observations of flows in excess of 2 km/s extending from 5 to 13 MLT. Previous studies of intense energy deposition and fast-flow channels under strong IMF B_Y conditions only observed local "hot spots" of a few hundred kilometers in ionospheric Joule heating that coincided with fast flows observed by the DMSP spacecraft [*Crowley et al*., 2010; *Wilder et al*., 2012b]. The inclusion of Sondrestrom incoherent scatter radar data as well as AMPERE FAC data in addition to DMSP shows that these fast flows can cover a wide range of MLT, extending over more than a quarter of the zonal circumference. This should have significant consequences in generating enhanced ionospheric Joule heating under IMF B_Y-dominant conditions and the associated thermospheric neutral density upheaval.

[13] Further, the temporal response of the high-latitude ionospheric convection and large-scale FAC system was investigated. It was found that in addition to the propagation delay between solar wind observations and the associated geophysical effects, there was also a delay exceeding 1 h between the peak IMF B_Y and the peak dawnside FAC and dayside ionospheric flow. This time lag is important for two reasons. First, it is very close to the auto-correlation lag between a southward turning of the IMF and the maximum auroral electrojet index value [*Arnoldy et al*., 1971]. Second, under southward IMF, this lag is associated with the reconfiguration time of the magnetosphere during a substorm growth and expansion phase [*Baker et al*., 1996, and references therein]. Additionally, the peak in the dawnside FACs coincides with the four-sheet pattern observed by AMPERE during the reconfiguration of FACs shown in Figure 2. Therefore, Figures 2 and 4 suggest a sequence of events as follows. First, when the IMF B_Y component turns strongly negative, magnetic reconnection is initiated in the morning sector close to the cusp, driving the cusp FAC pair, as well as fast ionospheric flows and open magnetic flux transport from the near-dawn flank to the nightside of the magnetosphere. This open flux builds up in the tail, skewed towards the dawn sector due to the IMF B_Y. Additionally, as field lines become open, they have the possibility to reconnect with the IMF or with closed field lines, leading to complex topologies as outlined by *Watanabe and Sofko* [2008, 2009]. Eventually, open flux tubes in the tail near the dawn sector will reconnect, enhancing the dawnside Region 1 and 2 FAC pair and driving fast ionospheric flows near MLT dawn in the ionosphere. This combination of different reconnection "types" can also lead to the four-sheet pattern observed in the morning sector in Figures 2 and 3. Eventually, the system relaxes and four-sheet system becomes significantly less prominent, and more like what one would traditionally expect under IMF B_Y-dominant conditions [*Watanabe and Sofko*, 2008, and references therein].

[14] The results of the present study demonstrate the challenges in predicting dayside energy deposition from the magnetosphere into the ionosphere during non-southward IMF. The fast flows associated with intense Joule heating can be found over a broader range of MLT than previously observed. Additionally, processes analogous to substorms under southward IMF may lead to a delay between a strong dawnward or duskward IMF turning and the peak FAC and convection seen in the morning or afternoon sector, respectively. While periods where the IMF B_Y component dominates are typically considered geomagnetically quiet, the present study shows that there is still significant activity, albeit at higher latitudes. Further work will be needed to determine what magnetospheric processes lead to the large amount of temporal variability in the FAC and convection patterns during these intervals.

[15] **Acknowledgments.** F. D. W.'s efforts were supported by the National Science Foundation Atmospheric and Geospace Sciences Postdoctoral Research Fellowship. S. E. was supported by NSF under grant AGS-1144154. Funding for processing the AMPERE data was provided by NSF under grant ATM-0739864. J. B. H. B. was supported by NSF under grants ATM-0946900 and AGS-1150789. M. R. H. was supported by NASA under LWS grant NNX07AT18G. C. H. and the Sondrestrom Facility were supported by the US National Science Foundation under cooperative agreement AGS-0836152.

[16] The Editor thanks William Bristow and two anonymous reviewers for their assistance in evaluating this paper.

References

Anderson, B. J., K. Takahashi, and B. A. Toth (2000), Sensing global Birkeland currents with iridium® engineering magnetometer data, *Geophys. Res. Lett.*, *27*(24), 4045–4048.

Anderson, B. J., S.-. I. Ohtani, H. Korth, and A. Ukhorskiy (2005), Storm time dawn-dusk asymmetry of the large-scale Birkeland currents, *J. Geophys. Res.*, *110*, A12220, doi:10.1029/2005JA011246.

Anderson, B. J., H. Korth, C. L. Waters, D. L. Green, and P. Stauning (2008), Statistical Birkeland current distributions from magnetic field observations by the Iridium constellation, *Ann. Geophys.*, *26*, 671–687, doi:10.5194/angeo-26-671-2008.

Angelopoulos, V. (2008), The THEMIS mission, *Space Sci. Rev.*, *141*, 5–34.

Arnoldy, R. L. (1971), Signature in the interplanetary medium for substorms, *J. Geophys. Res.*, *76*(22), 5189–5201.

Baker, D. N., T. I., Pulkkinen, T. I. Pulkkinen, V. Angelopoulos, W. Baumjohann, and R. L. McPherron (1996), Neutral line model of substorms: Past results and present view, *J. Geophys. Res.*, *101*(A6), 12,975–13,010.

Clauer, C. R., and E. Friis-Christensen (1988), High latitude dayside electric fields and currents during strong northward IMF: Observations and model simulation, *J. Geophys. Res.*, *93*, 2749–2757.

Cassak, P. A. (2011), Theory and simulations of the scaling of magnetic reconnection with symmetric shear flow, *Phys. Plas.*, *18*, 072106, doi:10.1063/1.3602859.

Clausen, L. B. N., J. B. H. Baker, J. M. Ruohoniemi, S. E. Milan, and B. J. Anderson (2012), Dynamics of the region 1 Birkeland current oval derived from the Active Magnetosphere and Planetary Electrodynamics Response Experiment (AMPERE), *J. Geophys. Res.*, *117*, A06233, doi:10.1029/2012JA017666.

Crowley, G., D. J. Knipp, K. A. Drake, J. Lei, E. Sutton, and H. Lühr (2010), Thermospheric density enhancements in the dayside cusp region during strong B_Y conditions, *Geophys. Res. Lett.*, *37*, L07110, doi:10.1029/2009GL042143.

Dungey, J. W. (1961), Interplanetary magnetic field and the auroral zones, *Phys. Rev. Lett.*, *6*, 47–48.

Eriksson, S., and L. Rastätter (2013), Alfvén Mach number and IMF clock angle dependence of sunward flow channels in the magnetosphere, *Geophys. Res. Lett.*, *40*, 1257–1262, doi:10.1002/grl50307.

Eriksson, S., M. R. Hairston, F. J. Rich, H. Korth, Y. Zhang, and B. J. Anderson (2008), High latitude ionosphere convection and Birkeland current response for the 15 May 2005 magnetic storm recovery phase, *J. Geophys. Res.*, *113*, A00A08, doi:10.1029/2008JA013139.

Friis-Christensen, E., K. Lassen, J. Wilhjelm, J. Wilcox, W. Gonzalez, and D. Coburn (1972), Critical component of the interplanetary magnetic field responsible for large geomagnetic effects in the polar cap, *J. Geophys. Res.*, *77*, 19, doi:10.1029/JA077i019p03371.

Knipp, D., S. Eriksson, L. Kilcommons, G. Crowley, J. Lei, M. Hairston, and K. Drake (2011), Extreme Poynting flux in the dayside thermosphere: Examples and statistics, *Geophys. Res. Lett.*, *38*, L16102, doi:10.1029/2011GL048302.

Korth, H., B. J. Anderson, H. U. Frey, and C. L. Waters (2005), High-latitude electromagnetic and particle energy flux during an event with sustained strongly northward IMF, *Ann. Geophys.*, *23*, 1295–1310, doi:10.5194/angeo-23-1295-2005.

Korth, H., B. J. Anderson, and C. L. Waters (2010), Statistical analysis of the dependence of large-scale Birkeland currents on solar wind parameters, *Ann. Geophys.*, *28*, 515–530.

Lavraud, B., and J. E. Borovsky (2008), Altered solar wind-magnetosphere interaction at low Mach numbers: Coronal mass ejections, *J. Geophys. Res.*, *113*, A00B08, doi:10.1029/2008JA013192

Li, W., D. Knipp, J. Lei, and J. Raeder (2011), The relation between dayside local Poynting flux enhancement and cusp reconnection, *J. Geophys. Res.*, *116*, A08301, doi:10.1029/2011JA016566.

Lühr, H., M. Rother, W. Kohler, P. Ritter, and L. Grunwaldt (2004), Thermospheric up-welling in the cusp region, evidence from CHAMP observations, *Geophys. Res. Lett.*, *31*, L06805, doi:10.1029/2003GL09314.

Ohtani, S. *et al*. (1995), Four large-scale field-aligned current systems in the dayside high-latitude region, *J. Geophys. Res.*, *100*(A1), 137–153, doi:10.1029/94JA01744.

Potemra, T. A. (1994), Source of large-scale Birkeland currents, in *Physical Signatures of Magnetospheric Boundary Layer Processes*, edited by J. A. Holtet and A. Egeland, pp. 3–27, Kluwer Academic, Dordrecht, Netherlands.

Redmon, R. J., W. K. Peterson, L. Andersson, E. A. Kihn, W. F. Denig, M. Hairston, and R. Coley (2010), Vertical thermal O^+ flows at 850 km in dynamic auroral boundary coordinates, *J. Geophys. Res.*, *115*, A00J08, doi:10.1029/2010JA015589.

Rich, F., and M. Hairston (1994), Large-scale convection patterns observed by DMSP, *J. Geophys. Res.*, *99*(A3), 3827–3844.

Spearman, C. (1904), The proof and measurement of association between two rings, *Am. J. Pysch.*, *15*, 72–101.

Stone, E., A. Frandsen, R. Mewaldt, E. Christian, D. Margolies, J. Ormes, and F. Snow (1997), The advanced composition explorer, *Space Sci. Rev.*, *86*(1-22), 1998.

Swisdak, M., M. Opher, J. F. Drake, and F. Alouani Bibi (2010), The vector direction of the interstellar magnetic field outside the heliosphere, *Ap. J.*, *710*, 2, doi:10.1088/0004-637X/710/2/1769.

Taguchi, S., M. Sugiura, T. Iyemori, J. D. Winningham, and J. A. Slavin (1993), Characterization of the IMF B_Y-dependent field-aligned currents in the cleft region based on DE 2 observations, *J. Geophys. Res.*, *98*(A2), 1393–1407, doi:10.1029/92JA01014.

Wanliss, J., and K. Showalter (2006), High-resolution global storm index: Dst versus SYM-H, *J. Geophys. Res.*, *111*(A2), doi:10.1029/2005JA011034.

Watanabe, M., and G. J. Sofko (2008), Synthesis of various ionospheric convection patterns for IMF By-dominated periods: Split crescent cells, exchange cells, and theta aurora formation, *J. Geophys. Res.*, *113*, A09218, doi:10.1029/2007JA012868.

Watanabe, M., and G. J. Sofko (2009), Dayside four-sheet field-aligned current system during IMF B_Y-dominated periods, *J. Geophys. Res.*, *114*, A03208, doi:10.1029/2008JA013815.

Waters, C. L., B. J. Anderson, and K. Liou (2001), Estimation of global field aligned currents using the iridium® system magnetometer data, *Geophys. Res. Lett.*, *28*(11), 2165–2168.

Wilder, F. D., G. Crowley, B. J. Anderson, and A. D. Richmond (2012a), Intense dayside Joule heating during the 5 April 2010 geomagnetic storm recovery phase observed by AMIE and AMPERE, *J. Geophys. Res.*, *117*, A05207, doi:10.1029/2012JA017547.

Wilder, F. D., G. Crowley, S. Eriksson, P. T. Newell, and M. R. Hairston (2012b), Ionospheric Joule heating, fast flow channels, and magnetic field line topology for IMF By-dominant conditions – Observations and comparisons with predicted reconnection jet speeds, *J. Geophys. Res.*, *117*, A11311, doi:10.1029/2012JA017914.

Yamauchi, M., R. Lundin, and J. Woch (1993), The interplanetary magnetic field B_Y effects on large-scale field-aligned currents near local noon: Contributions from cusp part and non-cusp part, *J. Geophys. Res.*, *98*(A4), 5761–5767, doi:10.1029/92JA02934.